Inhibition of Expression of the Type I G Protein-Coupled Receptor for Vasoactive Intestinal Peptide (VPAC1) by Hammerhead Ribozymes†

Nabila Jabrane-Ferrat,‡ Allan S. Pollock,§ and Edward J. Goetzl*,‡

Departments of Medicine and Microbiology−Immunology and Department of Medicine, Veterans Affairs Medical Center, University of California, San Francisco, California 94143-0711

Received April 18, 2000; Revised Manuscript Received June 13, 2000

ABSTRACT: Vasoactive intestinal peptide (VIP) is a neuromediator expressed widely in the nervous, gastrointestinal, respiratory, and immune systems. Two G protein-coupled receptors (GPCRs), designated VPAC1 and VPAC2, bind VIP with high affinity and transduce increases in [cyclic AMP]$_i$ and [Ca^{2+}]$_i$. As there are no potent VPAC1- or VPAC2-selective antagonists, a hammerhead ribozyme (Rz) strategy capable of in vivo application was adopted to inactivate individual domains of VPAC1. Three Rzs were designed to cleave mRNA encoding the amino terminus, the third intracellular loop, and the cytoplasmic tail of human VPAC1 and were introduced by transfection into HEK-293 cells expressing recombinant human VPAC1. Each Rz specifically degraded VPAC1 mRNA and down-regulated VPAC1 protein and VIP-binding activity, as assessed by ribonuclease protection assays, Western blots, and binding of ^{125}I-VIP. Rz-mediated down-regulation of VPAC1 was associated with up to 75% suppression of VIP signaling of increases in [cyclic AMP]$_i$ and [IP3]$_i$, and of cyclic AMP response element-luciferase reports. The Rz specific for the amino terminus inhibited VPAC1 expression and signaling to the greatest extent. VIP-evoked cellular responses thus appear to be proportional to the level of VPAC1 expression. Specific Rzs may be powerful tools for manipulating tissue-specific contributions of GPCRs in vitro and in vivo.

Vasoactive intestinal peptide (VIP)[1] is a 28 amino acid mediator, originally described as a transmitter and trophic factor in the nervous system (*1*). However, VIP activities now are known to extend to mediation of adhesion, migration, production of cytokines, proliferation, and survival of diverse cell types (*2, 3*). Macrophages, T lymphocytes, mast cells, specialized glandular cells, epithelial cells, smooth muscle cells, and fibroblasts are all responsive to VIP (*2, 4*). In chronic inflammation and immunologic reactions, VIP recruits leukocytes and acts with other immune mediators to enhance migration-related functions of leukocytes. Although VIP affects macrophages, mast cells, and granulocytes, the principal target in immune reactions is the T-cell (*2, 5*−*9*). Nanomolar concentrations of VIP induce T-cell migration through basement membranes and other connective tissues by increasing the expression of adhesive molecules, stimulating chemotaxis, and inducing secretion of specific matrix metalloproteinases (MMPs) (*10, 11*). VIP also modulates the production and secretion of several cytokines including IL-2, IL-4, IL-10, TNF-α, and γ-interferon (*12*−*14*). T-cell-dependent production of IgG and IgM is inhibited by VIP concentrations that concurrently enhance the production of IgA and IgE (*15*). VIP has been detected at nanomolar levels in different types of active inflammatory fluids, including bronchoalveolar lavage (BAL) after intratracheal antigen challenge of mice primed with T-cell-dependent antigens (*6*), and in human nasal secretions and BAL fluid during spontaneous attacks of allergic rhinitis and asthma (*4, 16*).

Many cells express one or both of two G protein-coupled receptors (GPCRs) for VIP, termed VPAC1 and VPAC2. These receptors are 49% identical in amino acid sequence and have similar ligand-binding specificities and signaling pathways, but exhibit complementary patterns of distribution in some tissues (*6, 8, 17*). However, functional studies show that VPAC1 and VPAC2 can mediate different or even opposing effects on T-cell functions (*8, 10, 11*). The lack of potent selective pharmacological antagonists and of highly bioavailable agonists for VPAC1 and VPAC2 has prevented specific assignment of many in vitro activities of VIP to one of the VPAC receptors. Similar problems have limited in vivo investigations of the individual contributions of each VPAC receptor. In the present study, VPAC1 binding of VIP and signal transduction were analyzed following hammerhead ribozyme (Rz)-based suppression of VPAC1 in HEK-293 cells.

Rz-based antisense inhibition strategies have been employed successfully in many settings to suppress expression of diverse proteins sufficiently that dependent biological functions were impaired significantly. Sequence-specific Rzs

† These studies were supported by Grants AI 29912 (E.J.G.) and DK 31398 (A.S.P.) from the National Institutes of Health.

* To whom correspondence should be addressed at UB8B, Box 0711, 533 Parnassus at 4th, University of California Medical Center, San Francisco, CA 94143-0711. Tel.: (415) 476-5339; Fax: (415) 476-6915; E-mail: egoetzl@itsa.ucsf.edu.

‡ Departments of Medicine and Microbiology−Immunology.

§ Department of Medicine.

[1] Abbreviations: VIP, vasoactive intestinal peptide; MMP, matrix metalloproteinase; GPCR, G protein-coupled receptor; VPAC1, type I VIP receptor; VPAC2, type II VIP receptor; BAL, bronchoalveolar lavage; CRE, cyclic AMP response element; GAPDH, glyceraldehyde-3-phosphate dehydrogenase; Rz, hammerhead ribozyme; RPA, ribonuclease protection assay.

10.1021/bi0008783 CCC: $19.00
Published on Web 07/19/2000

Chart 1

Name	Sequence	Target domain
Rz-257	GAUGAGGGcugaugaguccgugaggacgaaacAGGCCAAG	Amino-terminus
Rz-1001	UGAGUAUGcugaugaguccgugaggacgaaacUGCUGUCA	3rd intracellular loop
Rz-1231	CAGCCCAGcugaugaguccgugaggacgaaacGCCCUGCA	Carboxy-terminal tail

transcribed by single-copy retroviral vectors can selectively eliminate even proteins expressed constitutively at high levels (*18*). Thus, Rzs in a retroviral vector were designed to delineate the domains of native VPAC1 receptors which have the highest susceptibility to such antisense suppression, using constructs targeting the amino terminus, the third intracellular loop, and a cytoplasmic domain. The results presented demonstrate that the amino-terminal domain is a more effective target site for VPAC1-directed Rzs than the third intracellular loop or the cytoplasmic domain.

EXPERIMENTAL PROCEDURES

Ribozyme (Rz) Plasmid Construction. The sequence of mRNA encoding human VPAC1 was analyzed by the Mufold program to predict the most stable secondary structure and to select multiple functionally critical sites with target sequences susceptible to cleavage by hammerhead ribozymes (Rzs). Three such sites were identified, which have both stable mRNA secondary structure and a central GUC Rz cleavage sequence. Three Rz cassettes, which each contain a hammerhead sequence designed to cleave one GUC motif, were constructed as described (*18*) with distinctive specificity for sites in the ligand-binding domain (Rz-257), third intracellular loop (Rz-1001), and cytoplasmic tail (Rz-1231) of human VPAC1 (Chart 1). The ribozyme cassettes were subcloned in *Not*I, *Mlu*I sites of pLNCX2 vector (*18*, *19*). Ribonucleotides in stem II of each Rz were denoted by lowercase letters, and ribonucleotides complementary to those of human VPAC1 were assigned uppercase letters.

In vitro Rz catalytic activity was evaluated by analyzing cleavage of a partial-length sense mRNA transcript of VPAC1 containing the target site specific for each T7 RNA polymerase-synthesized Rz RNA transcript. [α-^{32}P]UTP was incorporated during transcriptional synthesis of the VPAC1 to allow visualization of digested transcripts. After digestion, fragments in each sample were resolved by 8 M urea−8% polyacrylamide gel electrophoresis and patterns analyzed by phosphoimaging of dried gels.

Preparation of DNA Fragments and Riboprobes. pVPAC1−330 (bp 1−330) and pVPAC1−1305 (bp 865−1305) of the human VPAC1 open-reading frame were amplified by PCR from human full-length VPAC1 cDNA subcloned in pGEM3Zf vector (Promega). Pairs of primers for pVPAC1−330 were 5′-GACCATGCGCCCGCCAAGTC-CGCTGCC-3′ and 5′-CCAGCCTTCGTCGG-TGCAGCT-GCGGCT-3′; and for pVPAC1−1305 were 5′-ATCAACTC-CTCACTGTGGTGG-ATCATA-3′ and 5′-GGAAACCT-GCGTGCTGCACGTGGCGCC-3′. As *Taq* DNA polymerase was used to generate VPAC1 cDNAs by PCR, both constructs were sequenced to ensure that no mutation had been introduced by PCR and to determine the orientation, using T7 and Sp6 primers. A 234 nt glyceraldehyde-3-phosphate dehydrogenase (GAPDH) cDNA fragment was subcloned in the antisense orientation in PCRII vector (pCRIIGAPDH) (Invitrogen). For riboprobe synthesis, pVPAC1−330 and pVPAC1−1305 plasmid cDNAs were linearized with *Xba*I and transcribed from the Sp6 promoter using the MAXIscriptTM system (Ambion, Austin, TX) in the presence of [α-^{32}P]UTP (New England Nuclear, Boston, MA) to generate 468 nt and 574 nt RNA transcripts. pCRIIGAPDH was used as internal control and generated a 300 nt riboprobe when transcribed from T7 promoter using synthetic RNA polymerases (Ambion) in the presence of [α-^{32}P]UTP. Riboprobes were gel-purified on a 4% polyacrylamide−urea denaturing gel and eluted with ammonium acetate buffer.

Cell Culture, Lipotransfection, and Reporter Assays. Human embryonic kidney HEK-293 cells expressing human VPAC1 (HEK-293-VPAC-1 cells) (*20*) were grown in 100 mm diameter tissue culture plates in Dulbecco's minimal essential medium (UCSF Cell Culture Facility) supplemented with 10% fetal bovine serum, L-glutamine, penicillin, and streptomycin at standard concentrations and 0.5 mg/mL Geneticin. Cells were plated 24 h before transfection in 100 mm dishes to establish 40−50% confluent monolayers, and each plate was transfected with 4 μg of plasmid DNA encoding one human VPAC1 Rz or with control plasmid lacking an insert, using lipofectamine according to the manufacturer's procedure. At 24 h post-transfection, HEK-293-VPAC-1 Rz transfectants were incubated for an additional 16 h in serum-free medium with or without a stimulus. For reporter assays, HEK-293-VPAC-1 cells were cotransfected with 100 ng of pCRE-Luc and 4 μg of Rz constructs in serum-free media. Cell lysates were assayed for luciferase activity as recommended by the manufacturer (Promega). Emitted light was quantified in a microplate luminometer (MicroLumatPlus, Berthold). All transfections were performed in triplicate or quadruplicate, and at least three experiments were conducted for each protocol.

RT-PCR Assessment of mRNA Encoding Each Rz. Total RNA was extracted by Trizol reagent (Gibco-BRL) from control- and Rz-transfected HEK-293-VPAC-1 cells. cDNAs were generated by reverse transcription of the RNA using SuperScript kit (Gibco-BRL) and used as template for the PCR reactions with the following oligonucleotide primer pairs: 5′-CCTGGCCAAGGTCAT-CCATGACAAC-3′ and 5′-TGTCATACCAGGAAATGAGCTTGAC-3′ for the internal control GAPDH, and 5′-GACCTCCATAGAAGA-CAC-3′ and 5′-CTGGGGACCATCTGTTCT-3′ for all Rz constructs. Standard PCR was performed with *Taq* DNA polymerase for 25 cycles. The resulting PCR products were resolved by agarose gel electrophoresis and visualized by ethidium bromide staining.

RNase Protection Assay. Cytoplasmic RNA was isolated from duplicate pools of HEK-293-VPAC-1 cells 48 h after transfection with Rzs, as described (*21*). RNase protection assays were performed using an Ambion RPAII kit with hybridization at 42 °C overnight according to the manufacturer's procedure; 2×10^4 cpm of VPAC or GADPH riboprobe was added to 10 μg of HEK-293-VPAC-1 transfectant-derived RNA, and the RNA−probe mixture was lyophilized and hybridized overnight at 42 °C prior to digestion with RNase. The RNA−RNA hybrids which resisted RNase were precipitated, dissolved in loading buffer, and denatured at 95 °C for 5 min. Components then were resolved in a 4% polyacrylamide−8 M urea denaturing gel

in TBE buffer for 2 h at 1400 V. After drying, gels were exposed to X-ray films at −70 °C with intensifying screens.

Quantification of Ligand Binding. Triplicate aliquots of (5×10^4)−(1×10^5) HEK-293-VPAC-1 Rz transfectants/mL were incubated with ^{125}I-VIP (NEN) in the presence of 0 and 1 μM unlabeled VIP for 30 min at 22 °C. Bound ^{125}I-VIP was separated from unbound by rapid centrifugation through a mixture of phthalate oils as previously described (*9*). Radioactivity was determined in a γ counter (United Technologies Packard).

Western Blot Analysis. HEK-293-VPAC-1 cells transfected for 48 h with a Rz-containing plasmid or control plasmid lacking an insert were washed 3 times with ice-cold phosphate-buffered saline and lysed for 30 min in 10 mM Tris-HCl (pH 7.6) with 5 mM EDTA, 50 mM NaCl, 30 mM sodium pyruvate, 50 mM NaF, 100 mM Na_3VO_4, 0.5% Triton X-100, 10 mg/mL leupeptin, 10 mg/mL aprotinin, and 1 mM phenylmethylsulfonyl fluoride. Lysates were clarified by centrifugation at 2000*g* for 10 min at 4 °C. Supernatants were collected, and proteins were separated under denaturing conditions on SDS−PAGE (10.5% polyacrylamide gel). Proteins were transferred to a nitrocellulose membrane and probed with either a monoclonal antibody to full-length human VPAC1 (Antibody Solutions, Inc., Palo Alto, CA) or a rabbit polyclonal antibody specific for peptide 54−70 in the extracellular amino terminus of VPAC2, which was prepared as for rabbit anti-VPAC1 antibodies (*22*). Mouse and rabbit IgG bound to VPAC1 and VPAC2, respectively, were detected using goat anti-mouse IgG conjugated to horseradish peroxidase alone or after reaction with mouse anti-rabbit IgG, and then development of chemiluminescence with luminol, as directed by the manufacturer (ECL Western, Amersham Pharmacia Biotech).

Determination of Intracellular Concentration of Cyclic AMP. Suspensions of 4×10^6 HEK-293-VPAC1 cells transfected with Rzs or control plasmid lacking an insert were harvested after 48 h and preincubated with 0.6 mM 3-isobutyl-1-methylxanthine (Calbiochem, San Diego, CA) and 20 μM Ro20−1724 (Sigma-Aldrich, St. Louis, MO) for 30 min at 22 °C prior to stimulation. Replicate aliquots of 5×10^5 HEK-293-VPAC-1 Rz-transfectants were treated with 1 μM VIP for an additional 30 min at 37 °C in 200 μL of phosphate-buffered saline supplemented with 1 g/100 mL of crystallized hen ovalbumin. The reaction was stopped by addition of 1 mL of ice-cold PBS, and cells were collected by centrifugation and lysed with 500 μL of absolute ethanol. Lyophilized supernatants were reconstituted in 50 mM sodium acetate buffer at pH 6.2 for quantification of $[cAMP]_i$ levels by enzyme-linked immunoassay according to the manufacturer's procedure (Perspective Diagnostics, Cambridge, MA).

Analysis of Inositol Phosphate Hydrolysis. Twenty-four hours after transfection with Rz or control plasmid, suspensions of 4×10^6 HEK-293-VPAC1 cells were labeled for 16 h with [^{3}H]myoinositol (5 mCi/mL) (NEN) at 37 °C in serum-free medium. The labeled cells were harvested, washed in HBSS−HEPES (pH 7.4) containing 0.1 g of bovine serum albumin/100 mL, divided into replicate suspensions of 2×10^6 cells/mL, and stimulated with VIP in the presence of 10 mM LiCl and 0.1 g/100 mL of bovine serum albumin for 30 min at 37 °C. Reactions were stopped by addition of 1 mL of ice-cold 6% trichloroacetic acid, samples were cleared by centrifugation, and the supernatants were extracted twice with 2 volumes of diethyl ether. Total [^{3}H]inositol phosphate in the lysate was retained on a Dowex AG-1-X8 column, and the radioactivity in eluates was quantified by β-scintillation counting.

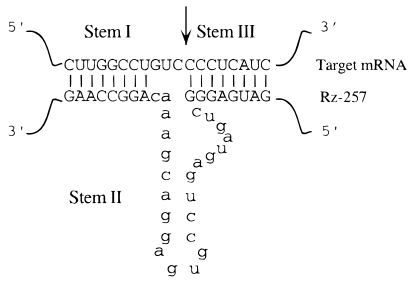

FIGURE 1: Sites of interaction of hammerhead ribozyme Rz-257 with VPAC1 mRNA in a three-stem structure. The upper sequence is VPAC1 target mRNA in the 5′-3′ orientation, and the lower sequence is Rz-257 RNA in the 3′-5′ orientation, which hybridizes to the G(257)UC triplet. The arrow points to the site of cleavage following the GUC triplet. The ribozyme nucleotides necessary for effective cleavage are indicated in lower case letters, and those constituting complementary flanking sequences for specific hybridization are indicated in upper case letters.

RESULTS

A series of three hammerhead ribozymes (Rzs) was constructed to target separately the extracellular amino terminus, implicated in ligand binding, and the third intracellular loop and cytoplasmic carboxy-terminal tail, involved in signaling by human VPAC1. Each Rz was introduced by transfection into HEK-293 cells stably expressing recombinant human VPAC1 (HEK-293-VPAC-1 cells) to determine their relative effectiveness in down-regulating VPAC1 expression and VPAC1-mediation of VIP-evoked signals. A schematic representation of the secondary structure of Rz RNA directed to $GU_{257}C$ in the amino terminus of the human VPAC1 mRNA sequence illustrates properties of these Rzs (Figure 1). Rz sequences were inserted as double-stranded oligonucleotides into the *Mlu*I, *Not*I cloning sites of pLNCX vector, so that each Rz sequence was under the control of the bacterial T7 promoter and an internal CMV promoter.

Catalytic Activity of VPAC1 Rzs. To demonstrate that the Rzs cleave VPAC1 mRNA, the catalytic activity of Rz transcripts was assessed with defined segments of human VPAC1 transcripts generated from two different VPAC1 cDNAs. pVPAC1−330, which contained the first 330 nt of the VPAC1 cDNA open-reading frame, and pVPAC1−1305, which contained 440 nt from nt 865 to nt 1305 of the VPAC1 open-reading frame, and plasmids encoding Rz sequences were used to transcribe from the T7 promoter the respective sense target RNA products p330 (468 nt) and p865 (574 nt), and each corresponding Rz. Incubation of pVPAC1−330 transcript with Rz-257 RNA resulted in generation of two cleavage products with the predicted molecular weights of 333 and 135 bp (Figure 2, arrows). Similarly, incubation of pVPAC1−1305 transcript with Rz-1001 RNA yielded two cleavage products with predicted molecular weights of 356 and 218 bp, whereas Rz-1231 RNA generated products of 448 and 126 bp (Figure 2, arrows). Increases in the ratio of Rz to target RNA from 10:1 to 50:1 resulted in total cleavage of the target RNA, but the background signals were much higher (data not shown). No cleavage was observed with

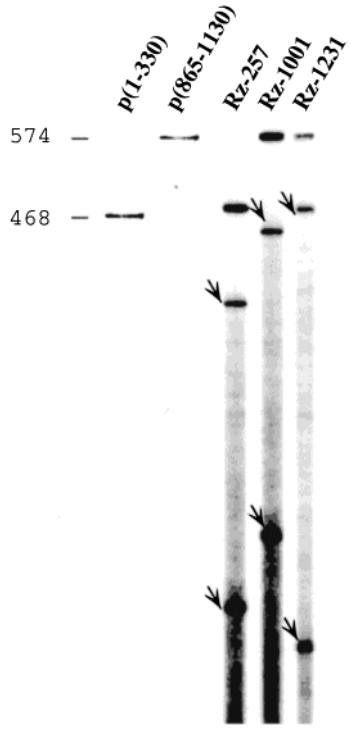

FIGURE 2: Ribozyme cleavage of human VPAC1 RNA transcripts. Coding inserts of the pVPAC1−330 (1−330) 468 nt included 1−330 and pVPAC1−1305 (865−1305) 574 nt included 865−1305. Each VPAC1 plasmid construct was transcribed from the SP6 promoter, and the respective [α-^{32}P]UTP-labeled riboprobes, termed p(1−330) (lane 1) and p(865−1305) (lane 2), were incubated with one of the ribozymes. The third lane (Rz-257) shows p(1−330) digested with Rz-257; the fourth lane (Rz-1001) is p865 digested with Rz-1001; and the fifth lane (Rz-1231) has p865 digested with Rz-1231. The cleavage fragments of the respective transcripts in each lane are indicated by arrows.

VPAC2 Rz (data not shown). These data indicate that T7 RNA polymerase-synthesized RNA transcripts of Rzs are active and selective in cleaving synthetic human VPAC1 transcripts.

Rz Delivery into the Cells. To elucidate the effects of VPAC1 Rzs in cells, the three constructs were introduced into HEK-293-VPAC1 cells by lipotransfection. The level of expression of Rz in HEK-293-VPAC-1 transfectants was assessed 48 h later by isolation of cytoplasmic RNA and RT-PCR analysis using primers that annealed to pLNCX vector sequences. A 177 bp cDNA was amplified from Rz-transfected HEK-293 cells, but not from control plasmid DNA transfected HEK-293-VPAC1 cells (Figure 3). The lack of generation of cDNAs by PCR without RT confirmed the principal source to be mRNA transcripts and not the cDNAs of the Rz plasmids.

Effect of VPAC1 Rzs on the Cellular Level of VPAC1 Expression. To investigate whether the cellular level of mRNA encoding VPAC1 was suppressed by Rzs, HEK-293-VPAC1 cells were transiently transfected with each of the Rz constructs, and mRNA transcripts were measured using RNase protection analyses (RPAs). RPAs revealed that expression of each Rz led to a decrease in VPAC1 mRNA (Figure 4A, compare lane 1 to lanes 2−4). Of the three Rzs, Rz-257 resulted in the greatest decrease of the protected band (Figure 4A and Figure 4B for quantification). The VPAC1-protected band is of the predicted molecular weight (330 nt). In contrast, levels of the control GAPDH mRNA reflected

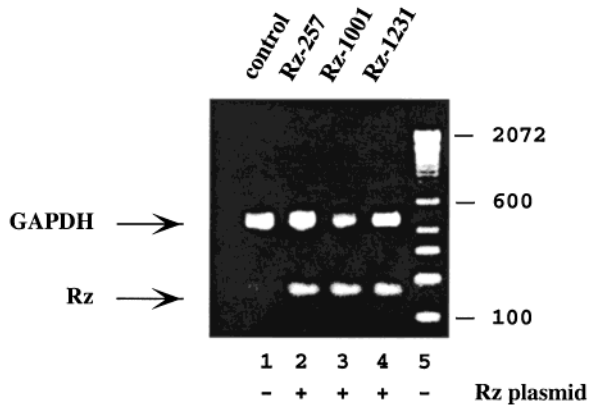

FIGURE 3: RT-PCR detection of ribozyme RNA in HEK-293 transfectants. Each lane contains PCR-amplified cDNA from cells transfected with control insert-free plasmids (lane 1), cells transfected with Rz-257-encoding plasmid construct (lane 2), cells transfected with Rz-1001 plasmid (lane 3), cells transfected with Rz-1231 plasmid (lane 4), and molecular weight markers (lane 5). Arrows point to the respective positions of specific GAPDH and Rz bands.

in a 234 nt protected band were not altered by the expression of any of the Rzs (Figure 4A, bottom band, lanes 1−4).

To confirm suppression of VPAC1 by Rzs, as suggested by the finding of lower mRNA levels in the RPAs, ligand binding was quantified in HEK-293-VPAC1 cells transfected with VPAC1-directed and control Rzs. No effect on the binding of ^{125}I-VIP by HEK-293-VPAC1 cells was observed 48 h after transfection with control Rz. In contrast, up to 75% reduction of total binding was attained in cells transfected with Rz-257, and 50% reduction was observed for Rz-1001- and Rz-1231-transfected cells (Figure 5A). Western blot analyses were carried out with protein extracts from HEK-293 transfectants. As shown in Figure 5B, VPAC1-specific Rz expression resulted in a significant decrease of VPAC1 protein, but no effect on VPAC2 expression.

These data together suggest that Rz expression resulted in substantial down-regulation of the level of VPAC1 expression in HEK-293 cells, that was greater for the Rz directed to the amino-terminal sequence than to those designed to target the intracellular loop or carboxy terminus.

Effect of VPAC1 Down-Regulation on Signaling. Since Rz expression resulted in specific reduction in the level of VPAC1 mRNA and protein, as well as binding of VIP, it was next determined whether this level of VPAC-1 suppression was reflected in decreased VIP-induced cellular signaling transduced by VPAC1. The main secondary messengers of VPAC1 signaling from VIP are (i) activation of adenylyl cyclase by coupling to Gs α subunit, resulting in increases in $[cAMP]_i$, and (ii) activation of phospholipase C, resulting in increases in diacylglycerol and inositol triphosphate, and consequently $[Ca^{2+}]_i$. Intracellular concentrations of cAMP and IP3 thus were quantified in HEK-293 cells stimulated by VIP after transfection with Rzs.

VIP has been shown to increase within minutes the level of cyclic AMP in cells that express VPAC1, with sustained increases for up to 30 min by stimulation of adenylyl cyclase. HEK-293-VPAC1 cells were stimulated with VIP for 30 min, 48 h after transfection with Rzs. VIP treatment of cells transfected with control plasmid induced a mean of 146-fold increase in the intracellular concentration of cAMP. The expression of Rzs down-regulated by over 60% the cAMP

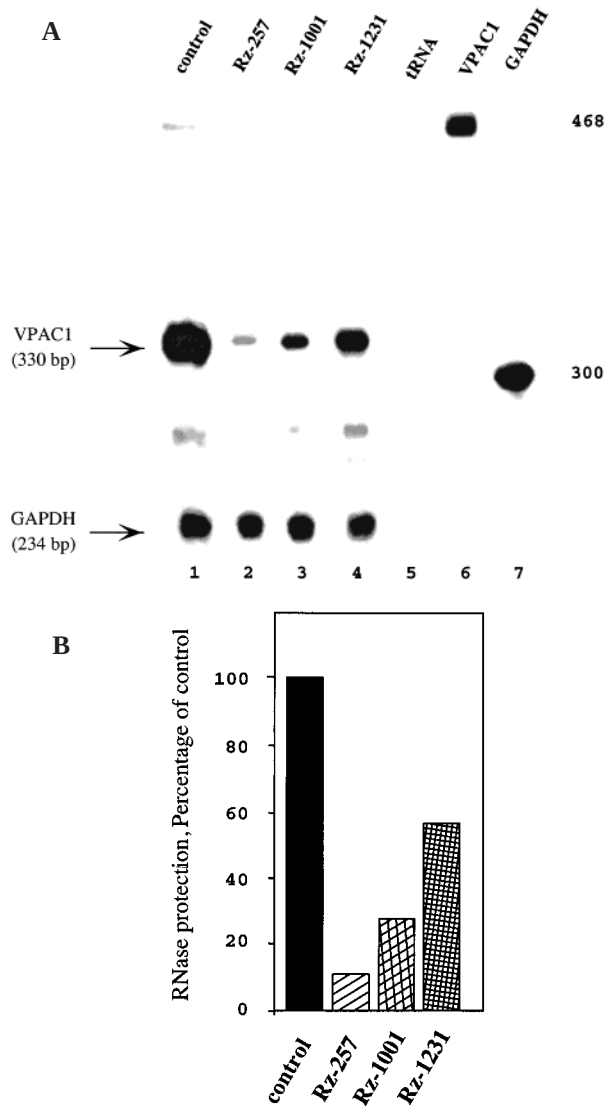

FIGURE 4: RNase protection assay of Rz-altered VPAC1 transcripts. (A) RNA from Rz-transfected HEK-293 cells expressing VPAC-1 was incubated with the [α-^{32}P]UTP-labeled 468 nt riboprobe, designated p(1−330), and the [α-^{32}P]UTP-labeled 300 nt riboprobe containing GAPDH234, followed by treatment with RNase. The protected fragments were analyzed by gel electrophoresis. Cells had plasmids encoding no Rz (control) (lane 1), Rz-257 (lane 2), Rz-1001 (lane 3), or Rz-1231 (lane 4). Lane 5 shows probes incubated with yeast tRNA; lane 6, VPAC1 probe (468 nt) alone; lane 7, GAPDH probe (300 nt) alone. Arrows point to the position of 330 nt protected band for VPAC1 (top) and the 234 nt protected band for GAPDH (bottom). (B) The intensities of each protected band in (A) were quantified using ImageQuant software and reported as a percentage of control after normalization to the GAPDH internal control. Decreases in percentage of control reflect increases in Rz activity.

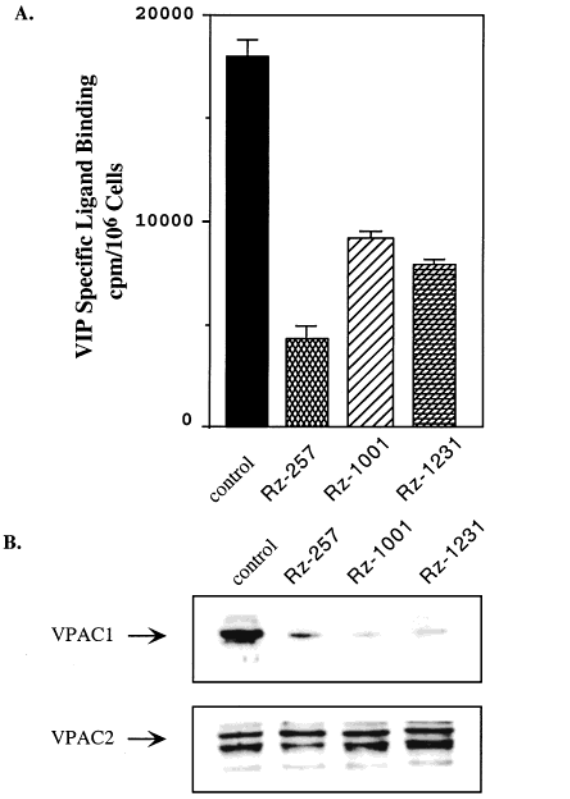

FIGURE 5: Quantification of Rz-induced suppression of expression and signaling of VPAC1. (A) Ligand binding. Results show decreases in specific binding of ^{125}I-VIP by HEK-293-VPAC1 cells. The bar graph depicts the specific binding of ^{125}I-VIP by 1×10^6 HEK-293-VPAC1 transfectants after introduction of control plasmid, Rz-257, Rz-1001, or Rz-1231. Each value represents the mean ± SEM of three different experiments performed in triplicate. (B) Western blot analysis of Rz-induced decreases in expression of VPAC1 by HEK-293-VPAC1 transfectants. Five micrograms of protein extracted from control, Rz-257, Rz-1001, and Rz-1231 plasmid-transfected cells was separated on a polyacrylamide gel under denaturing conditions. Blots were developed with mouse anti-human VPAC1 (top panel) monoclonal antibody or with rabbit anti-VPAC2 peptide polyclonal antibody (bottom panel). Arrows point to the positions of VPAC1 and VPAC2.

level attained in HEK-293-VPAC1 cells transfected with control plasmid (Figure 6A). The level of reduction in $[cAMP]_i$ correlated with decreases in VPAC1, as Rz-257 had the greatest effect. No Rz modification of the lesser response to forskolin was seen at any time after introduction of Rzs.

The level of metabolism of IP3 was quantified in HEK-293-VPAC1 cells by conversion of [^{3}H]myoinositol. VIP significantly enhanced IP3 levels by over 6-fold. The increase of IP3 evoked by VIP was much less in Rz-transfected cells with reduced expression of VPAC1. The increments were reduced to 1.7-, 2.7-, and 3.6-fold, respectively, by Rz-257, -1001, and -1231 (Figure 6B). Thus, activation of PLC was reduced when the level of VPAC1 was suppressed. Rz-257 again was the most effective of the Rzs.

Functional Relevance of cAMP Increases. Increases in the intracellular concentration of cAMP result in downstream up-regulation of CREB protein, that then binds and activates transcription from a CRE element. A reporter construct consisting of the CRE promoter element driving the expression of luciferase reporter gene was used to detect this cAMP-dependent effect of VIP in HEK-293 cells. The HEK-293-VPAC1 cells were cotransfected with pCRE-luciferase reporter construct and each Rz or control plasmid. Twenty-four hours after transfection, the cells were stimulated for an additional 12 h with VIP or forskolin (FSK) and compared to unstimulated cells. VIP induced a mean increase in luciferase activity of 47-fold in control HEK-293-VPAC1 cells. The increase in luciferase activity was reduced in Rz-transfected HEK-293-VPAC1 cells (Figure 7). As for other VIP-induced signals, Rz-257 transfectants attained only an 18-fold increase in luciferase activity while Rz-1001 and Rz-1231 reached 29- and 24-fold respective increases in lu-

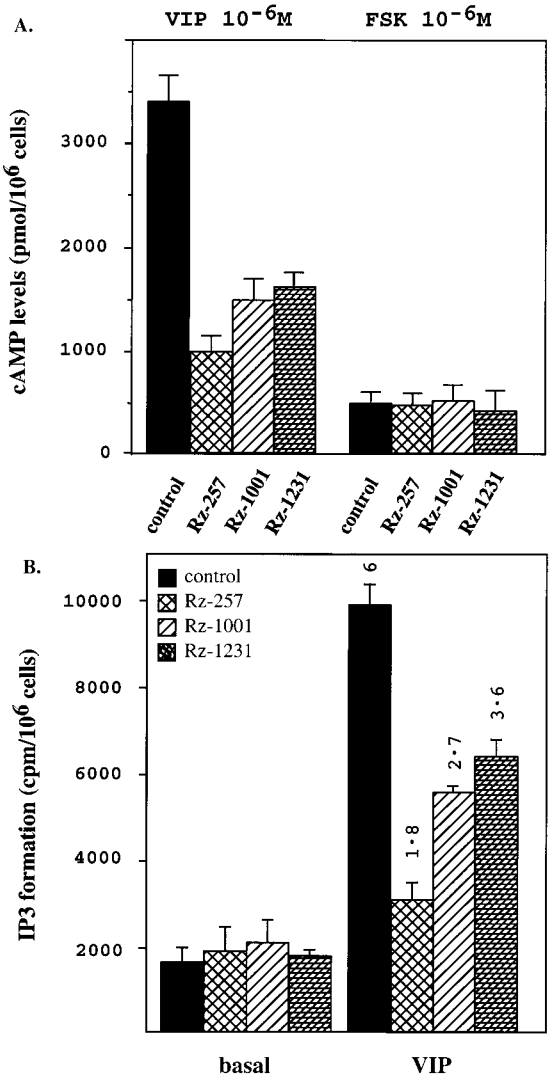

FIGURE 6: Specific suppression of VIP-evoked increases in $[cAMP]_i$ and $[IP3]_i$ by Rz-induced decreases in expression of VPAC1 in HEK-293-VPAC1 transfectants. (A) Each bar and bracket shows the mean effect (±SEM) of VIP or forskolin on $[cAMP]_i$ in three different experiments performed in triplicate with control and Rz-transfected cells. The number above each bar represents the magnitude of that response expressed as a percentage of the respective control VIP- or forskolin-evoked control (100%). (B) Each bar and bracket shows the mean level of formation of IP3 (±SEM) with buffer alone (basal) or 10^{-6} M VIP in three different experiments performed in triplicate with control and Rz-transfected HEK-293-VPAC1cells. The number above each experimental bar represents the mean fold-activation for that response calculated relative to the respective basal level (1.0).

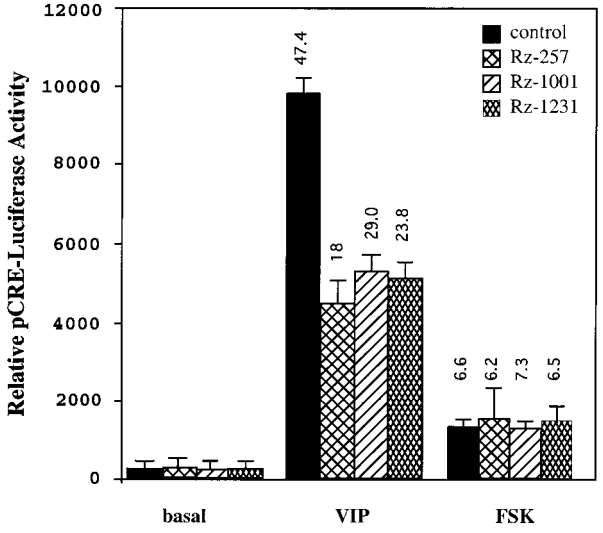

FIGURE 7: Suppression of VIP-evoked increases in pCRE-luciferase activity in HEK-293-VPAC1 cells. Each Rz suppressed expression of VPAC1 in HEK-293-VPAC1 cells. Each bar and bracket shows the mean relative pCRE-luciferase activity (±SEM) with buffer alone (basal), 10^{-6} M VIP, or 10^{-6} M forskolin in three different experiments performed in triplicate with control and Rz-transfected cells. The number above each bar represents the mean fold-activation for that response calculated relative to the respective basal level (1.0).

ciferase activity. No effect of Rzs was observed when the cells were activated by forskolin.

DISCUSSION

Many of the physiological roles of VIP are only partially understood because of difficulties in deleting genes encoding VIP or receptors for VIP with organ system selectivity and a lack of potent pharmacological antagonists. HEK-293 cells stably expressing human recombinant VPAC1 receptors represent a model system for elucidating both approaches to and consequences of altered expression of VPAC1. Hammerhead ribozymes (Rzs) act as site-specific ribonucleases which cleave target RNA and successfully inhibit the expression of targeted genes (*23, 24*). A Rz-based strategy thus was selected for targeting specific sequences of VPAC1 mRNA in HEK-293-VPAC1 transfectants to identify the domains which endow susceptibility to Rz antisense inhibition of expression and functions of native VPAC1 receptors. A retroviral vector-based delivery system was employed as described (*18*), since this system ensures efficient cellular expression of the Rz after transfection, and also permits ready adaptation to in vivo applications.

Each of three different ribozymes was highly expressed in HEK-293 transfectants (Figure 3) and effectively targeted VPAC1 RNA, as assessed by RNA cleavage (Figure 2). Rz-257, that cleaved mRNA encoding the extracellular amino terminus, suppressed to the greatest extent expression of VPAC1 receptors, as assessed by reduction of the levels of mRNA, VPAC1 protein in Western blot analyses, and binding of ^{125}I-VIP (Figures 4 and 5). Rz effects were specific for VPAC1 since there were no effects on VPAC2 expression in HEK-293 transfectants. The inhibition of VPAC1 expression correlated with suppression of VIP-mediated signaling (Figures 6 and 7). VIP-induced increases in $[cAMP]_i$ were decreased by the introduction of each Rz (Figure 6). The extent of suppression of VIP-induced increases in $[cAMP]_i$ correlated with the degree of reduction in the levels of expression of VPAC1. Rz-257, which reduced VPAC1 levels the greatest, had the most prominent suppressive effect on VIP-evoked increases in $[cAMP]_i$ levels (Figure 6). Similarly, the extent of Rz inhibition of VIP-induced accumulation of IP3 and increases in CRE-luciferase reports correlated with the degree of reduction in expression of VPAC1 by HEK-293 cells (Figures 6 and 7). Rz expression had no impact on FSK-mediated stimulation of adenylyl cyclase, which supported the specificity of Rz actions on VPAC1 rather than signaling events.

Results of studies of rat VPAC1 and secretin receptor chimeras demonstrated a dominant role of the extracellular amino terminus in VIP binding affinity and specificity (*25*).

Our demonstration of the effectiveness of Rz-257 in suppressing VPAC1 expression and signaling in parallel provides the first evidence that the extracellular amino terminus of VPAC1 is a prominent target for Rz-mediated suppression of VPAC1 expression in plasma membranes, as well as its VIP-binding activity. However, the relative capacity of each Rz to inhibit expression of VPAC1 does not provide an adequate basis for definition of the importance of that domain in VPAC expression and signaling. Residual expression of 25−45% of VPAC1 receptors by HEK-293-VPAC1 cells appears to be sufficient to mediate VIP signaling and elicitation of cellular responses. As HEK-293 transfectants express approximately 10^6 recombinant VPAC1 receptors per cell (*20*), in contrast to only up to 10^5 native receptors per cell for most tissues, however, it is possible that Rzs will have far greater suppressive effects on VIP-mediated signaling and VIP-mediated function in situ and in vivo. Rzs thus may be valuable reagents for selective targeting of specific organ systems in investigations complementary to transgenic overexpression with tissue-selective promoters.

REFERENCES

1. Said, S., and Mutt, V., Eds. (1988) *Vasoactive Intestinal Peptide and Related Peptides*, New York Academy of Sciences, New York.
2. Goetzl, E. J., and Sreedharan, S. P. (1992) *FASEB J. 6*, 2646−2652.
3. Gressens, P., Paindaveine, B., Hill, J. M., Brenneman, D. E., and Evrard, P. (1997) *Ann. N.Y. Acad. Sci. 814*, 152−160.
4. Mosimann, B. L., White, M. V., Hohman, R. J., Goldrich, M. S., Kaulbach, H. C., and Kaliner, M. A. (1993) *J. Allergy Clin. Immunol. 92*, 95−104.
5. Johnston, J. A., Taub, D. D., Lloyd, A. R., Conlon, K., Oppenheim, J. J., and Kevlin, D. J. (1994) *J. Immunol. 153*, 1762−1768.
6. Kaltreider, H. B., Ichikawa, S., Byrd, P. K., Ingram, D. A., Kishiyama, J. L., Sreedharan, S. P., Warnock, M. L., Beck, J. M., and Goetzl, E. J. (1997) *Am. J. Respir. Cell Mol. Biol. 16*, 133−144.
7. Xia, M., Gaufo, G. O., Wang, Q., Sreedharan, S. P., and Goetzl, E. J. (1996) *J. Immunol. 157*, 1132−1138.
8. Xia, M., Sreedharan, S. P., and Goetzl, E. J. (1996) *J. Clin. Immunol. 16*, 21−30.
9. Xia, M., Sreedharan, S. P., Bolin, D. R., Gaufo, G. O., and Goetzl, E. J. (1997) *J. Pharmacol. Exp. Ther. 281*, 629−633.
10. Xia, M., Leppert, D., Hauser, S. L., Sreedharan, S. P., Nelson, P. J., Krensky, A. M., and Goetzl, E. J. (1996) *J. Immunol. 156*, 160−167.
11. Xia, M., Sreedharan, S. P., Dazin, P., Damsky, C. H., and Goetzl, E. J. (1996) *J. Cell. Biochem. 61*, 452−458.
12. Sun, L., and Ganea, D. (1993) *J. Neuroimmunol. 48*, 59−69.
13. Jabrane-Ferrat, N., Bloom, D., Wu, A., Li, L., Sreedharan, S. P., Turck, C. W., and Goetzl, E. J. (1999) *FASEB J. 13*, 347−353.
14. Delgado, M., Pozo, D., Martinez, C., Leceta, J., Calvo, J. R., Ganea, D., and Gomariz, R. P. (1999) *J. Immunol. 162*, 2358−2367.
15. Hassner, A., Lau, M. S., Goetzl, E. J., and Adelman, D. C. (1993) *J. Allergy Clin. Immunol. 92*, 891−901.
16. Goetzl, E. J., Pankhaniya, R. R., Gaufo, G. O., Mu, Y., Xia, M., and Sreedharan, S. P. (1998) *Ann. N.Y. Acad. Sci. 840*, 540−550.
17. Usdin, T. B., Bonner, T. I., and Mezy, E. (1994) *Endocrinology 135*, 2662−2680.
18. Turck, J., Pollock, A. S., Lee, L. K., Marti, H. P., and Lovett, D. H. (1996) *J. Biol. Chem. 271*, 15074−15083.
19. Miller, A. D., Miller, D. G., Garcia, J. V., and Lynch, C. M. (1993) *Methods Enzymol. 217*, 581−599.
20. Sreedharan, S. P., Patel, D. R., Xia, M., Ichikawa, S., and Goetzl, E. J. (1994) *Biochem. Biophys. Res. Commun. 203*, 141−148.
21. Lim, C. S., Jabrane-Ferrat, N., Fontes, J. D., Okamoto, H., Garovoy, M. R., Peterlin, B. M., and Hunt, C. A. (1997) *Nucleic Acids Res. 25*, 575−581.
22. Goetzl, E. J., Patel, D. R., Kishiyama, J. L., Smoll, A. C., Turck, C. W., Law, N. M., Rosenzweig, S. A., and Sreedharan, S. P. (1994) *Mol. Cell. Neurosci. 5*, 145−152.
23. Lan, N., Howrey, R. P., Lee, S.-W., Smith, C. A., and Sullenger, B. A. (1998) *Science 280*, 1593−1596.
24. Murray, J. B., Terwey, D. P., Maloney, L., Karpeisky, A., Usman, N., Beigelman, L., and Scott, W. G. (1998) *Cell 92*, 665−673.
25. Couvineau, A., Rouyer-Fessard, C., Maoret, J.-J., Gaudin, P., Nicole, P., and Laburthe, M. (1996) *J. Biol. Chem. 271*, 12795−12800.

BI0008783